Review Article

Imaging of the pituitary: Recent advances

Vikas Chaudhary, Shahina Bano[1]

Department of Radiodiagnosis, Employees' State Insurance Corporation (ESIC) Model Hospital, Gurgaon, Haryana, [1]Govind Ballabh (GB) Pant Hospital and Maulana Azad Medical College, New Delhi, India

ABSTRACT

Pituitary lesions, albeit relatively infrequent, can significantly alter the quality of life. This article highlights the role of advanced imaging modalities in evaluating pituitary-hypothalamic axis lesions. Magnetic resonance imaging (MRI) is the examination of choice for evaluating hypothalamic-pituitary-related endocrine diseases. Advanced MR techniques discussed in this article include dynamic contrast-enhanced MRI, 3T MRI, magnetization transfer (MT) imaging, diffusion-weighted imaging (DWI), proton MR spectroscopy, fluorine-18 fluorodeoxyglucose-positron emission tomography, single-photon emission computed tomography, intraoperative MRI, and intraoperative real-time ultrasonography.

Key words: Computed tomography, imaging, magnetic resonance imaging, pituitary, recent advances

Introduction

Pituitary gland plays a central role in body growth, metabolism, and reproductive function. A number of diseases that affect the pituitary-hypothalamic axis can have profound clinical, endocrinological as well as neurological consequences. These conditions can be classified as neoplastic, infectious, inflammatory, posttraumatic, congenital/developmental, and physiological. Various neoplastic conditions include pituitary adenoma/apoplexy, hypothalamic glioma, craniopharyngioma, rathke cleft cyst, germinoma, teratoma, metastasis, leukemic infiltration, lymphoma, and Langerhans cell histiocytosis. Infectious and inflammatory causes include tubercular/lymphocytic hypophysitis, sarcoidosis, and Wegener's granulomatosis. Traumatic causes include postoperative sella or transection of the pituitary stalk. Accurate diagnostic differentiation of these lesions is essential for both safe and effective disease management. Recent advances in neuroimaging helps the radiologists and endocrinologists to study the pituitary region in greater detail. Magnetic resonance imaging (MRI) is the imaging modality of choice for evaluating hypothalamic-pituitary-related endocrine diseases.

Access this article online	
Quick Response Code:	Website: www.ijem.in
	DOI: 10.4103/2230-8210.84871

Normal Anatomy and Applied Physiology

The sellar region is an anatomically complex area bounded by sphenoid sinus anteroinferorly, the paired cavernous sinuses laterally, the suprasellar cistern and its contents, diaphragma sellae and hypothalamus superiorly, and the dorsum sella and brainstem posteriorly.[1]

The hypothalamus is a layer of tissue extending from the anterior commissure to the posterior commissure. The inferior ridge of tissue from the optic chiasma to the mamillary bodies is called the tuber cinereum. The hypothalamus consists of multiple nuclei regulating the temperature, water balance, drinking behavior, and sexual activity. The hypothalamus and the pituitary gland are functionally and physiologically interlinked contiguous structures and often referred to as the hypothalamic-pituitary axis. Oxytoxin and vasopressin are synthesized in the hypothalamus and transported to the posterior pituitary.[2]

Corresponding Author: Dr. Vikas Chaudhary, Department of Radiodiagnosis, Employees' State Insurance Corporation (ESIC) Model Hospital, Gurgaon – 122 001, Haryana, India. E-mail: dr_vikaschaudhary@yahoo.com

The pituitary gland is composed of two anatomically and functionally distinct lobes: the anterior lobe (adenohypophysis) and the posterior lobe (neurohypophysis).[3] The anterior lobe comprises 75% of volume of the gland and consists of pars tuberalis (part of the infundibular stalk and median eminence of hypothalamus), pars intermedia (a vestigial structure and common site for developmental cyst) and pars distalis (forms most part of intrasellar adenohypophysis).[4] Rathke's pouch is the embryologic precursor of the anterior pituitary gland which usually regresses during early fetal development. Occasionally, its remnant persists into the postnatal life and gives rise to a macroscopic cyst, the Rathke cleft cyst.[5] The adenohypophysis does not have direct arterial supply. It receives its blood principally from the hypophyseal-portal system, which also serves as a pathway for release of hypothalamic hormones.[6] The hormones produced and secreted by the anterior lobe include growth hormone (GH), adrenocorticotropic hormone (ACTH), prolactin (PRL), thyroid stimulating hormone (TSH), luteinizing hormone (LH), and melanocyte-stimulating hormone (MSH).[7] The anterior lobe of pituitary is isointense to cortical brain on both T1-weighted and T2-weighted images.[3]

The posterior pituitary lobe, infundibular stalk, supraoptic, and paraventricular hypothalamic nuclei form the neurohypophysis. The oxytocin and vasopressin, synthesized in the hypothalamus, are transported along the hypothalamo-hypophyseal tract to the posterior lobe and stored there. The posterior lobe appears as a bright spot on T1-weighted images.[1,8] Neurosecretory vesicles are responsible for high signal intensity of the posterior pituitary lobe.[9] The absence of high signal is often associated with central diabetes insipidus or compressive pituitary gland lesions.[10,11]

The dimensions of pituitary glands are highly variable, particularly its height. The gland undergoes dramatic changes in size and shape throughout life. A useful guide to the gland's height in relation to age is "Elster's rule" of 6,8,10,12: 6 mm for infants and children, 8 mm in men and postmenopausal women, 10 mm in women of childbearing age and 12 mm for women in late pregnancy or postpartum women.[1] The pituitary stalk has a normal thickness of 2 mm, and it should not exceed a maximum of 4 mm or the width of the basilar artery.

Imaging Modalities

Pituitary imaging is important not only in confirming the diagnosis of pituitary lesions but also in determining the differential diagnosis of other sellar lesions. Plain skull radiographs are poor at delineating soft tissues, and infrequently requested these days for diagnosing sellar and parasellar pathologies. The radiographic size of sella is not a sensitive indicator of pituitary gland abnormality, as the empty sella may itself lead to enlargement of size.[12] Thus the plain radiographs have been replaced by cross-sectional imaging techniques such as CT scanning and MRI.

CT scan, though less frequently used for evaluating sellar and parasellar lesions, is a useful examination depicting soft tissue calcification, bony destruction, and surgically relevant bony anatomy. CT scans are valuable, particularly when MRI is contraindicated, such as in patients with pacemakers or metallic implants in the brain or eyes. However, less optimal soft tissue contrast and radiation exposure are two important drawbacks that limit the judicious use of CT scan for evaluating pituitary lesions.

Currently, MRI is the examination of choice for sellar and parasellar pathologies due to its superior soft tissue contrast, multiplanar capability and lack of ionizing radiation. In addition, MRI also provides useful information about the relationship of the gland with adjacent anatomical structures and helps to plan medical or surgical strategy. MRI techniques in diagnosing pituitary lesions have witnessed a rapid evolution, ranging from noncontrast MRI in late 1980s to contrast-enhanced MRI in mid-1990s. Introduction of dynamic contrast-enhanced MRI has further refined this technique in diagnosing pituitary microadenomas.[13] Recently, a variety of advanced MR techniques have been evolved which are particularly helpful in evaluating specific cases. These include 3D volumetric analysis of pituitary volume,[14] high-resolution MR imaging at 3 Tesla (T) for evaluating pituitary stalk,[15] diffusion-weighted imaging,[16] MR spectroscopy,[17] magnetization transfer ratio,[18] and intraoperative MRI.[19]

The aim of MR imaging is to obtain a high-spatial-resolution image with a reasonable signal to noise ratio. It is important to identify the gland separate from the lesion if possible. Initially, precontrast T1- and T2-weighted spin echo coronal and sagittal sections are acquired using a small FOV (20×25 cm), thin slices (3 mm), and high-resolution matrix (256×512). Both the dynamic and routine postcontrast images and delayed scanning after 30-60 minutes may be combined in one study for optimum imaging.

Although most adenomas are detected on nonenhanced MRI, microadenomas may become visible only after contrast injection. Dynamic contrast MRI has been proven to be the best imaging tool in the evaluation of pituitary adenomas. A three-dimensional Fourier transformation gradient echo or fast turbo spin echo sequence (TSE) may be used for dynamic study. A dose of 0.05 mmol/kg of gadolinium injected intravenously is usually adequate. After a bolus injection of intravenous gadolinium, six consecutive sets of three images are obtained in coronal plane every 10 seconds. The enhancement occurs first in the pituitary stalk, then in the pituitary tuft (the junction point of the stalk and gland), and finally there is centrifugal opacification of the entire anterior lobe. Within 30-60 seconds the entire gland shows homogenous enhancement. The maximum image contrast between the normal pituitary tissue and microadenomas is attained about 30-60 seconds after the bolus injection of the intravenous contrast. Most microadenomas appear as relatively nonenhancing (dark) lesions within an intensely enhancing pituitary gland [Figures 1 and 2].[13] The peak enhancement of the pituitary adenomas occurs at 60-200 seconds, usually after the most marked enhancement of the normal pituitary gland, and persists for a longer duration.[14] Delayed scan (30-60 minutes after contrast injection) may demonstrate a reversal of the image contrast obtained at 30-60 seconds on dynamic scanning. This is because the contrast from the normal pituitary gland fades but diffuses into the microadenoma which stands out as a hyperintense focus.[15] Yuh *et al*.[16] have documented early enhancement in the microadenomas, long before the anterior lobe, which is attributed to pituitary adenomas having a direct arterial blood supply similar to that of posterior pituitary lobe.[17] Addition of dynamic sagittal plane images to the routine coronal study increases the overall detection rate of pituitary microadenomas.[18] Dynamic contrast MRI is not only useful in evaluating the pituitary microadenomas but also has an equally important role in assessing the macroadenomas, invasion of cavernous sinus by the macroadenomas, and differentiating residual/recurrent tumor from postoperative tissues.[16-18] Some microadenomas exhibit maximum lesion-to-gland contrast on unenhanced scan; however, this image contrast begins to diminish the moment the contrast-enhancing agent arrives in the pituitary gland.

Pituitary insufficiency with a sellar or suprasellar mass lesion is certainly suggestive of a nonsecretory pituitary tumor, which cannot be differentiated clinically from lymphocytic hypophysitis (LH). In any woman presenting with a sellar mass lesion during pregnancy or in the first postpartum year, LH should be suspected, though it can be diagnosed with certainty only histologically. MR imaging is currently the best noninvasive diagnostic tool to differentiate lympohocytic hypophysistis (LH) from nonsecreting macroadenomas, although no single radiological feature is characteristic of the disease. MR features indicative of LH include symmetric enlargement of the gland, homogeneous appearance, intense contrast enhancement, thickening and enhancement of the pituitary stalk, loss of posterior pituitary bright spot, and enhancement of dura adjacent to the pituitary mass and an intact sellar floor. In contrast, pituitary macroadenomas are frequently asymmetric, usually heterogeneous in appearance, have lesser gadolinium uptake, rarely involves the stalk, preservation of posterior pituitary bright spot and eroded sellar floor. Although, a thickened pituitary stalk is typical for LH and strongly favors LH over adenoma, an enlarged pituitary stalk can be found in a variety of diseases, such as germinoma,

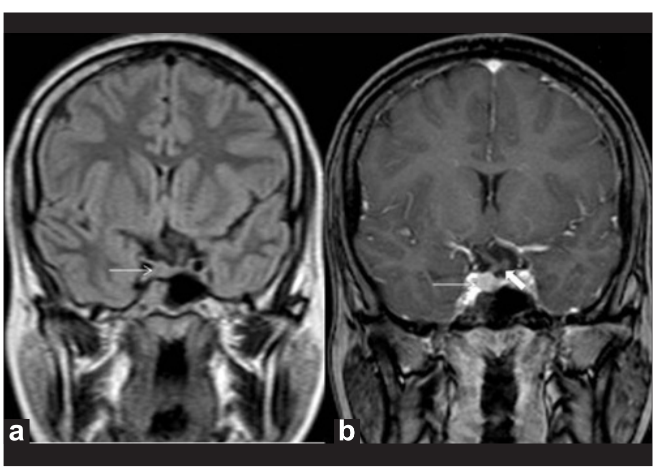

Figure 1: Pituitary microadenoma. Coronal fluid attenuated inversion recovery (a) and routine T1-weighted postcontrast (b) images of brain show a small nodular lesion (thin white arrow) involving the right side of the pituitary gland producing mild bulge of superior margin of the gland and leftward deviation of the pituitary stalk (thick white arrow). The lesion appears isointense to the gland on the fluid attenuated inversion recovery image and shows an enhancement pattern almost identical to the normal pituitary gland

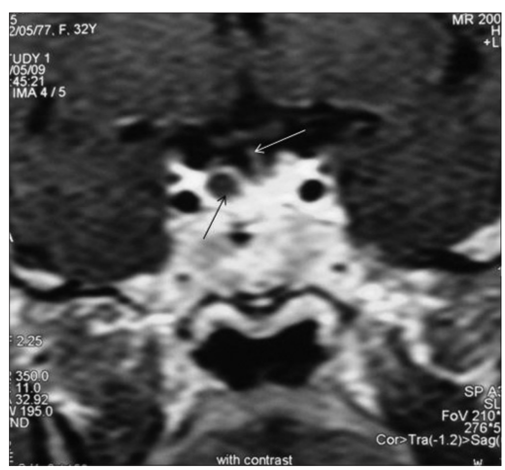

Figure 2: Pituitary microadenoma. High-resolution dynamic contrast-enhanced T1-weighted coronal image of brain of another patient (at 60 seconds) shows a small nonenhancing (dark) microadenoma (thin black arrow) lateralized to the right side of the pituitary gland. Note that the lesion is more conspicuous on dynamic contrast scan compared to the routine contrast scan (seen in figure 5b). The normal pituitary gland shows marked homogenous enhancement and there is no deviation of pituitary stalk (thin white arrow) in this case

lymphoma, tuberculosis, sarcoidosis, or Langerhans cell histiocytosis, but its presence in the absence of systemic infections suggests a diagnosis of hypophysitis. Hence, MR imaging increases the probability of diagnosing LH and plays a very important role in the management of patients with LH, who are benefited more from medical as opposed to surgical treatment. Until a specific antibody for this disease or a characteristic MR feature has been identified, the diagnosis of this entity must rely only on the histologic study.[20]

3-Tesla MRI with stronger magnetic field strength offers an improved image quality and spatial resolution under conditions with subtle differences between normal and abnormal tissue. A recent study has shown that preoperative localization of pituitary microadenomas in Cushing's disease is relatively better with 3T MRI compared to 1.5T MRI, although some of these lesions were missed even on 3T MRI.[21] Wolfsberger *et al*.[22] used 3T MRI to study the invasion of cavernous sinus by the adenomas in 42 patients. They found that 3T MRI using T1-weighted magnetization prepared rapid acquisition gradient echo (MPRAGE) sequence provides a superior delineation of cavernous sinus invasion by intrasellar tumors compared with standard MRI techniques. However, they did not compare 3T MRI with 1.5T MRI with respect to a specific tumor type. The role of 3T MRI is under an evolutionary stage and needs further refinement with use of newer sequences for confirming the presence of microadenomas that do not produce contour abnormalities, and identifying their number and location within the gland as these pieces of information are very useful in planning the surgical management of pituitary microadenomas in Cushing's disease. Moreover, the knowledge of normal pituitary gland volume and normal imaging appearance of the pituitary stalk is important for diagnosing different lesions of the gland and infundibulum. Accurate assessment of the stalk and subtle changes in gland volume is better with 3T MRI than with 1.5 T MRI.[23,24]

Although pituitary adenomas can be well delineated on plain and contrast-enhanced MR sequences, the differentiation between secreting and nonsecreting adenomas is not possible using classical MRI. In addition, the role of MRI in evaluating residual tumor in postoperated cases is also limited. Magnetization transfer (MT) imaging is a recent advancement in the field of imaging which can be used for preoperative and postoperative assessment of pituitary adenomas in patients with hyperprolactinemia. In MT imaging, the tissue contrast depends mainly on the concentration of macromolecules, and is quantified by the magnetization transfer ratio (MTR). In patients with hyperprolactinemia, the MTR of prolactin-secreting adenomas is significantly higher, compared to the MTR value of normal pituitary gland in the controlled group, as a result the prolactin-secreting adenomas having high signal on MT images. Contrary to this, the nonsecreting adenomas have lower MTR compared to that of normal pituitary gland and demonstrate low signal on MT images. The differentiation between these two types of pituitary adenomas is important because they are managed separately. Most cases of prolactinomas are treated medically, while nonsecreting adenomas are managed surgically. The MT technique can also be used in postoperative assessment and follow-up of patients with pituitary adenomas, especially when classical MRI is negative for residual tumor. Increased MTR values are highly suggestive of persistent adenomatous tissue. Future prospect of MT imaging includes other pituitary disorders such as pituitary insufficiency and precocious puberty.[25] The role of diffusion-weighted imaging (DWI) in early detection of acute pituitary infarction has been evaluated by some authors. Pituitary apoplexy which results from either hemorrhage or infarction of the pituitary gland may be associated with high mortality and morbidity. It has been documented that DWI assists in the early diagnosis of acute pituitary infarction with timely intervention and excellent outcome. On imaging, pituitary infarction may be diagnosed by the presence of peripheral contrast enhancement of an intrasellar mass on contrast-enhanced images and restricted water diffusion within these lesion on DW images. Acute pituitary infarction on DWI may mimic pituitary hemorrhage, abscess, and hypophysitis.[26] Diffusion-weighted imaging and apparent diffusion coefficient (ADC) maps can characterize tumor components within microadenomas and provide information about the consistency of macroadenomas. Most microadenomas are soft and easily resectable using a minimally invasive endoscopic transsphenoidal technique, whereas 10% macroadenomas with increased fibrosis are hard and difficult to be removed by the endoscopic technique and may require more extensive surgery. Thus, the knowledge of consistency of macroadenomas may help the clinician to plan a proper surgical technique for resection. On MRI, soft macroadenomas [Figure 3] appear inhomogeneous and hyperintense or isointense on T2WI, hypointense on T1WI and exhibit marked contrast enhancement on the postgadolinium image. These lesions demonstrate a high signal intensity on DWI and have a low ADC value of $(0.663 \pm 0.109) \times 10^{-3}$ mm^2/sec. Macroadenomas in the intermediate group [Figure 4] appear inhomogenous and hyperintense on T2WI, iso- or hypointense on T1WI and exhibit marked enhancement after administration of intravenous contrast agent. On DWI, these lesions demonstrate a high signal intensity, however having a ADC value higher than that for soft adenomas and lower

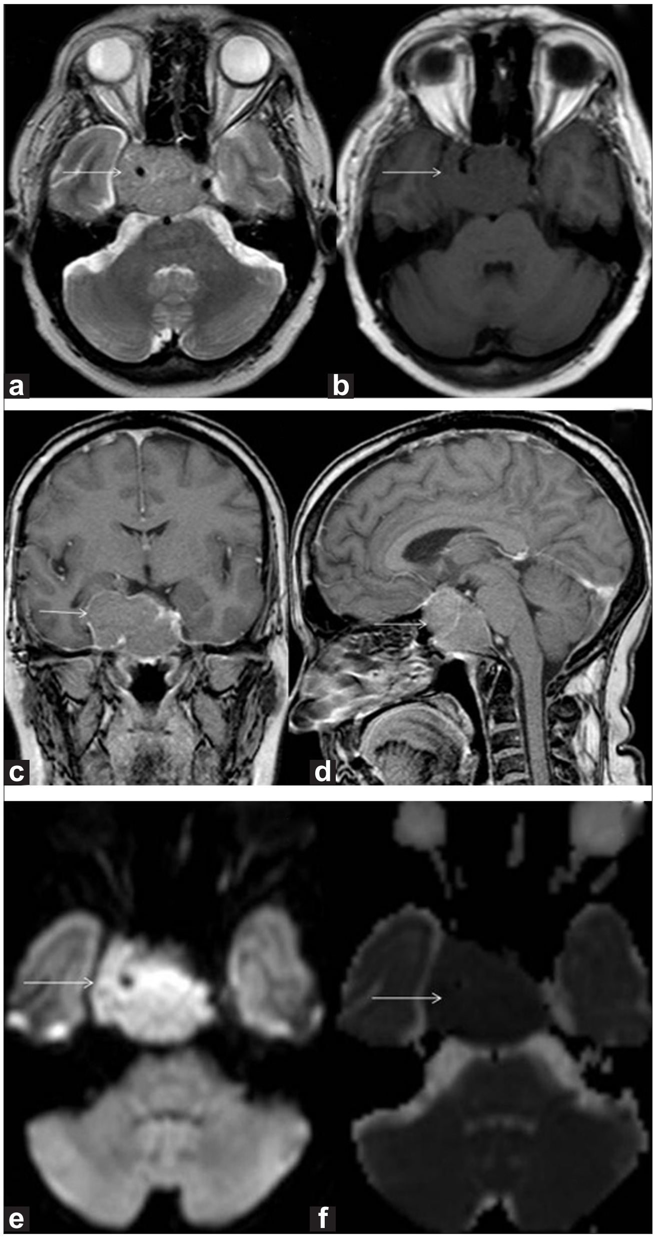

Figure 3: Pituitary macroadenoma with soft consistency. Axial T1W (a) and T2W (b) images show a large inhomogeneous, T1- and T2W isointense pituitary mass (arrow), encroaching bilateral cavernous sinus regions. On postcontrast coronal (c) and sagittal (d) images, the lesion exhibits moderate contrast enhancement. Left internal carotid artery (the cavernous part) appears to be displaced laterally by the mass, while the right internal carotid artery is seen traversing through the mass, which also shows invasion of ipsilateral cavernous sinus. However, both the arteries demonstrate normal contrast opacification with mild luminal compromise. On diffusion-weighted image (e) the lesion is hyperintense to the brain and has a low ADC value compared to normal brain parenchyma, $(0.566 \pm 0.109)\times10^{-3}$ mm^2/sec on apparent diffusion coefficient mapping (f)

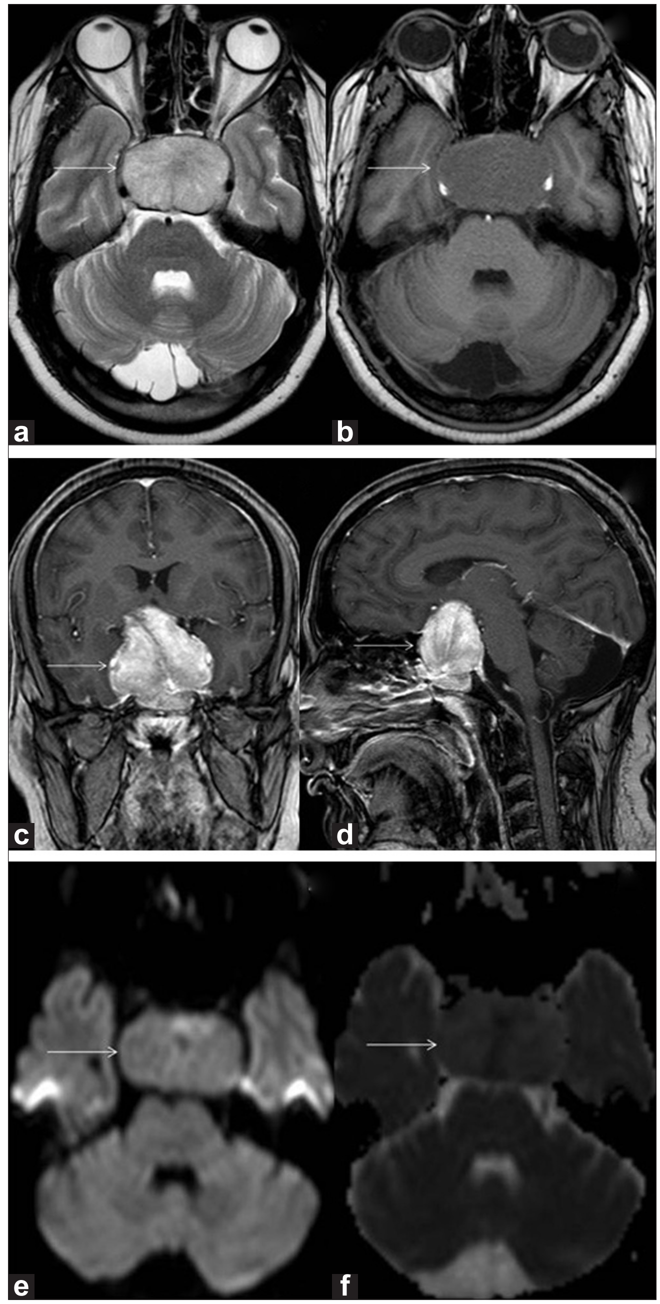

Figure 4: Pituitary macroadenoma with intermediate consistency. Axial T1W (a) and T2W (b) images show a large inhomogeneous, T1-hypointense and T2-hyperintense pituitary mass (arrow), which causes a lateral displacement of bilateral internal carotid arteries (cavernous part). On postcontrast coronal (c) and sagittal (d) images, the lesion exhibits marked but heterogeneous contrast enhancement. On the diffusion-weighted image (e) the lesion is isointense to the brain with an ADC value similar to that of normal brain parenchyma, $(0.872 \pm 0.138)\times10^{-3}$ mm^2/sec on apparent diffusion coefficient mapping (f)

than that for hard adenomas $(0.842\pm0.081) \times 10^{-3}$ mm^2/sec. Hard macroadenomas [Figure 5] are inhomogeneous and hyperintense on T2WI, hypointense on T1WI, and exhibit marked enhancement on intravenous contrast administration. These tumors demonstrate a low signal intensity on DWI and have a relatively high ADC value of $(1.363\pm0.259) \times 10^{-3}$ mm^2/sec. DWI should become a part of routine assessment of macroadenomas for planning the surgical approach.[26]

Proton MR spectroscopy can be helpful in differentiating various types of lesions involving pituitary-hypothalamic

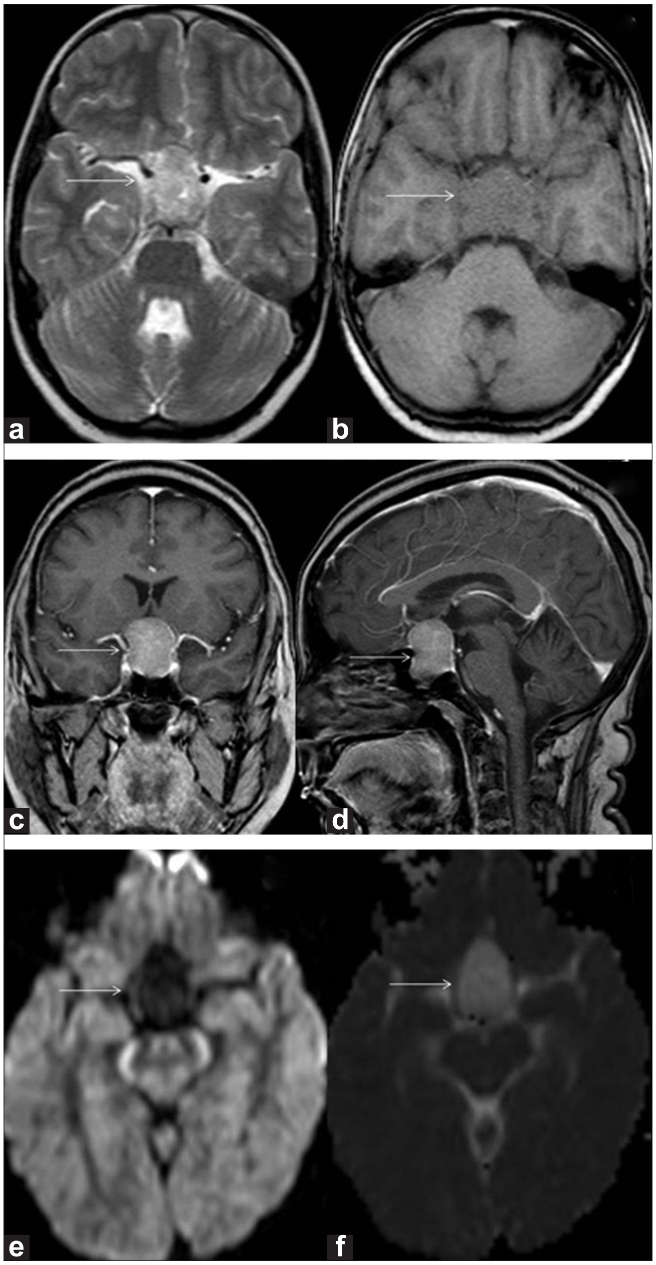

Figure 5: Pituitary macroadenoma with hard consistency. Axial T1W (a) and T2W (b) images demonstrat a large inhomogeneous, T1-hypointense, T2-hyperintense pituitary mass (arrow), which shows marked enhancement on postcontrast coronal (c) and sagittal (d) images. On the diffusion-weighted image (e) the lesion is profoundly hypointense to the brain and shows a high apparent diffusion coefficient value $(1.412 \pm 0.125)\times10^{-3}$ mm^2/sec on corresponding apparent diffusion coefficient mapping (f)

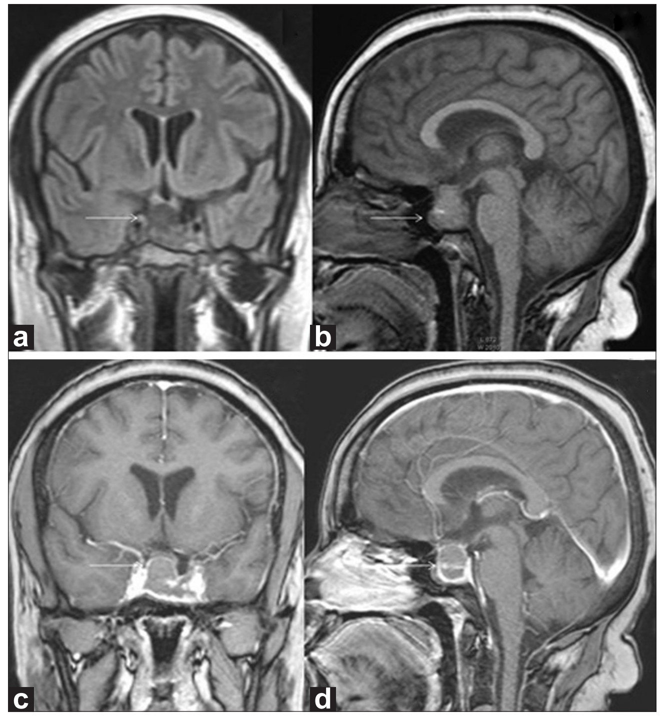

Figure 6: Pituitary macroadenoma with hemorrhage. Axial T1W (a) and T2W (b) images reveal a pituitary mass (arrow) showing intratumoral hemorrhage. On postcontrast coronal (c) and sagittal (d) images, the lesion demonstrates mild enhancement with left cavernous sinus invasion. Proton MR spectroscopy shows prominence of lipid-lactate peak with reduction of all other metabolites

axis. Proton MR spectroscopy of hypothalamic gliomas show increased choline and decreased *N*-acetyl aspartate while craniopharyngiomas and germiomas show a dominant lipid peak.[27,28] Pituitary adenomas [Figure 6] may show only a choline peak or no metabolites at all in the case of intratumoral hemorrhage (as hemosiderin worsens the magnetic field homogeneity).[29] MR spectroscopy findings of hypothalamic hamartomas include decreased *N*-acetyl aspartate and increased myoinositol compared to gray matter.[30]

Although MRI remains the method of choice for evaluation of pituitary tumors, there are several situations in which positron emission tomography (PET) scanning has the potential to provide valuable clinical information in the assessment of pituitary tumors. Fluorine-18 fluorodeoxyglucose-positron emission tomography (FDG-PET) can be used to differentiate residual or recurrent tumor from postoperative changes or radiation injury. An increased uptake of FDG is observed in the case of residual/recurrent tumors, whereas the postoperative changes or radiation injuries show decreased uptake of FDG. FDG-PET can also be used to differentiate macroadenomas from other sellar and suprasellar masses. Macroadenomas are identified as foci of increased FDG uptake near the region of sella. Uptake of FDG is highest in nonfunctional adenomas.[18] FGD-PET is also useful in staging and monitoring the disease and better treatment planning.[31,32]

The role of single-photon emission computed tomography (SPECT) using iodine 123 labeled dopamine D2 receptor antagonist iodobenzamide (IBZM) in evaluating pituitary tumors is not very promising. A study done on 15 patients with pituitary tumors showed a poor sensitivity of IBZM-SPECT to visualize prolactin and growth hormone secreting macroadenomas in general.[33]

The most recent advancement in pituitary imaging is the use of intraoperative MRI (IMRI) and intraoperative real-time ultrasonography during endoscopic pituitary surgery. IMRI provides better visualization of intra- and parasellar anatomy facilitating complete resection of the tumor. IMRI using a plasma screen has a promising role in the near future as it can provide a sufficient high quality image to demonstrate the nerve compression and the residual tumor.[34] The use of intraoperative real-time ultrasonography has proven to be very useful in localizing the intracranial neoplasms, particularly the deep skull base lesions and facilitating their resection. It also assists in guiding needles for biopsy and aspiration of pituitary lesions.[35]

Thus, we conclude that MRI is the investigation of choice for evaluating hypothalamic-pituitary-related endocrine diseases. MRI not only helps in the diagnostic differentiation of these lesions but also provides useful information about the relationship of the gland with adjacent anatomical structures and helps to plan medical or surgical strategy. DWI should become a part of routine assessment of macroadenomas for planning the surgical approach.

References

1. Elster AD. Imaging of the sella: Anatomy and pathology. Semin Ultrasound CT MR 1993;14:182-94.
2. Carpenter MC. Core text of neuroanatomy. 2nd ed. Baltimore, MD: Williams and Wilkins; 1978. p. 216-35.
3. Johnsen DE, Woodruff WW, Allen IS, Cera PJ, Funkhouser GR, Coleman LL. MR imaging of the sellar and juxtasellar regions. Radiographics 1991;11:727-58.
4. Schwartzberg DG. Imaging of pituitary gland tumors. Semin Ultrasound CT MR 1992;13:207-23.
5. Crenshaw WB, Chew FS. Rathke's cleft cyst. AJR Am J Roentgenol 1993;158:1312.
6. Elster AD. Modern imaging of the pituitary. Radiology 1993;187: 1-14.
7. Schubiger O. Intrasellar tumors: Neuroradiological diagnosis. Riv Neuroradiol 1991;4:47-55.
8. Fujisawa I, Asato R, Nishimura K, Togashi K, Itoh K, Nakano Y, *et al*. Anterior and posterior lobes of pituitary gland, assessment by 1.5 MR imaging. J Comput Assist Tomogr 1987;11:214-20.
9. Mark LP, Haughton VM, Hendrix LE, Daniels DL, Williams AL, Czervionke LF, *et al*. High-intensity signals within the posterior pituitary fossa: A study with fat suppression MR techniques. AJNR Am J Neuroradiol 1991;12:529-32.
10. Colombo N, Berry I, Kucharczyk J, Kucharczyk W, de Groot J, Larson T, *et al*. Posterior pituitary gland: Appearance on MR imaging in normal and pathological states. Radiology 1987;165:481-5.
11. Sato N, Ishizaka H, Yagi H, Matsumoto M, Endo K. Posterior lobe of the pituitary in diabetes incipidus: Dynamic MR imaging. Radiology 1993;186:357-60.
12. Latchaw RE, Roppole HM. Radiographic evaluation of the normal sella turcica and the pituitary gland. In Radiological Diagnosis Imaging Intervention. Vol 3. Philadelphia: JB Lippincott Co; 1986. p. 1-7.
13. Cheemum L, Walter K, Walter JM, Laurence EB. The sella turcica and parasellar region. In Magnetic resonance imaging of the brain and spine. Vol 2. Philadelphia: WW Lippincott Co; 2002. p. 1283-362.
14. Sakamoto Y, Takahashi M, Korogi Y, Bussakhi H, Ushio Y. Normal and abnormal pituitary glands: Gadopentate dimeglumine enhanced MR imaging. Radiology 1997;178:441-5.
15. Dwyer AJ, Frank JA, Doppman JL, Oldfield EH, Hickey AM, Cutler GB, *et al*. Pituitary adenomas in patients with cushing disease: Initial experience with GD-DTPA-enhanced MR imaging. Radiology 1987;163:421-6.
16. Yuh WT, Fisher DJ, Nguyen HD, Tali ET, Gao F, Simonson TM, *et al*. Sequential MR enhancement patterns in normal pituitary gland and in pituitary adenoma. AJNR Am J Neuroradiol 1994;15:101-8.
17. Boneville JF, Canthin F, Gorczyca W, Hardy J. Pituitary microsdenomas: Early enhancement with dynamic CT-implications of arterial blood supply and potential importance. Radiology 1993;187:857-61.
18. Gao R, Isoda H, Tanaka T, Inagawa S, Takeda H, Takehara Y, *et al*. Dynamic gadolinium enhanced MR imaging of pituitary adenomas: Usefulness of sequential sagittal and coronal plane images. Eur J Radiol 2001;39:139-46.
19. Scotti G, Yu CY, Dillon WP, Norman D, Colombo N, Newton TH, *et al*. MR imaging of cavernous sinus involvement by pituitary adenomas. AJR Am J Roentgenol 1988;151:799-806.
20. Gutenberg A, Larsen J, Lupi I, Rohde V, Caturegli P. A radiologic score to distinguish autoimmune hypophysitis from nonsecreting pituitary adenoma preoperatively. AJNR Am J Neuroradiol 2009;30:1766-72.
21. Louis JK, Gregory PL, William LW, John K. Preliminary experience with 3-Tesla MRI and cushing's disease. Skull Base 2007;17:273-7.
22. Wolfsberger S, Ba-Ssalamah A, Pinker K, Mlynárik V, Czech T, Knosp E, *et al*. Application of three-tesla magnetic resonance imaging for diagnosis and surgery of sellar lesions. J Neurosurg 2004;100: 278-86.
23. Satogami N, Miki Y, Koyama T, Kataoka M, Togashi K. Normal pituitary stalk: High resolution MR imaging at 3T. AJNR Am J Neuroradiol 2010;31:355-9.
24. Ikram MF, Sajjad Z, Shokh IS, Omair A. Pituitary gland volume on magnetic resonance imaging: Normative observations. Pak J Neurol Sci 2007;2:141-4.
25. Maria IA, Dimitrios NK. Magnetization transfer imaging of the pituitary gland. Hormones 2003;2:98-102.
26. Alberto P, Francesca C, Carlo F, Emanuele T, Amalia P, Alessia BC, *et al*. Pituitary macroadenomas: Preoperative evaluation of consistency with diffusion-weighted MR imaging-initial experience. Radiology 2006;239:223-31.
27. Sutton LN, Wang ZJ, Wehrli SL, Marwaha S, Molloy P, Phillips PC, *et al*. Proton spectroscopy of suprasellar tumors in pediatric patients. Neurosurgery 1997;41:388-94.
28. Kendi TK, Caglar S, Huvaj S, Bademci G, Kendi M, Alparslan S. Suprasellar germ cell tumor with subarachnoid seeding MR and MR spectroscopy findings. Clin Imaging 2004;28:404-7.
29. Stadlbauer A, Buchfelder M, Nimsky C, Saeger W, Salomonowitz E, Pinker K, *et al*. Proton magnetic resonance spectroscopy in pituitary macroadenomas: Preliminary results. J Neurosurg 2008;109:306-12.
30. Freedman JL, Coleman LT, Wellard RM, Kean MJ, Rosenfeld

JV, Jackson GD, *et al*. MR imaging and spectroscopic study of epileptogenic hypothalamic hamartomas: Analysis of 72 cases. AJNR Am J Neuroradiol 2004;25:450-62.
31. Muhr C, Bergstrom M. Positron emission tomography applied in study of pituitary adenomas. J Endocrinol Invest 1991;14:509-28.
32. De Souza B, Brunetti A, Fulham MJ, Brooks RA, Demichele D, Cook P, *et al*. Pituitary macroadenomas: A PET study. Radiology 1990;177:39-44.
33. Pirker W, Brücke T, Riedl M, Clodi M, Luger A, Asenbaum S, *et al*. Iodine -123-IBZM-SPECT: Studies in 15 patients with pituitary tumors. J Neural Transm Gen Sect 1994;97:235-44.
34. Theodore HS, Phillip ES, Vijay KA. Endoscopic transsphenoidal pituitary surgery with intraoperative magnetic resonance imaging. Neurosurgery 2006;58:44-51.
35. Atkinson JL, Kasperbauer JL, James EM, Lane JI, Nippoldt TB. Transcranial-transdural real-time ultrasonography during transsphenoidal resection of a large pituitary tumor. Case report. J Neurosurg 2000;93:129-31.

Cite this article as: Chaudhary V, Bano S. Imaging of the pituitary: Recent advances. Indian J Endocr Metab 2011;15:216-23.

Source of Support: Nil, **Conflict of Interest:** None declared.